Experimental-Numerical Correlation of a Multi-Body Model for Comfort Analysis of a Heavy Truck

2020-01-0768

Experimental-numerical correlation of a multi-body model for comfort analysis of a heavy truck

Author, co-author (Do NOT enter this information. It will be pulled from participant tab in MyTechZone)

Affiliation (Do NOT enter this information. It will be pulled from participant tab in MyTechZone)

Abstract

In automotive market, today more than in the past, it is very important to reduce time to market and, mostly, developing costs before the final production start. Ideally, bench and on-road tests can be replaced by multi-body studies because virtual approach guarantees test conditions very close to reality and it is able to exactly replicate the standard procedures. Therefore, today, it is essential to create very reliable models, able to forecast the vehicle behavior on every road condition (including uneven surfaces).

The aim of this study is to build an accurate multi-body model of a heavy-duty truck, check its handling performance, and correlate experimental and numerical data related to comfort tests for model tuning and validation purposes. Experimental results are recorded during tests carried out at different speeds and loading conditions on a Belgian blocks track. Simulation data are obtained reproducing the on-road test conditions in multi-body environment. The virtual vehicle is characterized by rigid and flexible bodies, the tire model used is FTire (Flexible Structure Tire Model) while the 3D scan of the road surface is imported using OpenCRG format. Signals coming from accelerometers, positioned on suspension axles, the truck chassis and cabin, are investigated both in time and frequency domain, using three different methods typical of random signals: the power spectral density (PSD) analysis, the root mean square (RMS) and the level crossing peak counting (LC). The good match between simulation and experimental data validates the adopted simulation methodology, therefore this work has provided a valuable tool for studies concerning comfort, NVH, durability and fatigue in order to improve safety and reliability of future heavy-duty vehicles.

Introduction

The commercial vehicles market is becoming very competitive in order to meet customers' demands. Clients, today, ask for products with high performances, high comfort, low fuel consumption and low price. Moreover, trucks are the vehicles that travel the highest number of kilometers every day and transport companies need to reduce the TCO (Total Cost of Ownership) in order to remain competitive in their sector. For this reason, to fulfil buyers' wants, OEMs must improve continuously their industrial vehicles and invest on research. Considering these factors, CAE is an essential tool for companies to reduce developing time and costs in comparison to the traditional method which consist in physical prototypes building and testing [1-3]. Virtual simulation allows to obtain great economic savings and time saving, but, at the same time, before "replacing" bench and on-road tests, it is mandatory to have reliable multi-body models.

Vehicle dynamics and comfort are becoming more and more important, mostly with regards to the safety of the driver, of passengers and of pedestrians. The purpose of vehicle dynamics is to guarantee a simple and predictable behavior of the running vehicle and can be considered integral part of the active safety. The aim of comfort is to improve the driving experience reducing motion sickness, vibrations and noise that could be annoying for human body.

Vibration can be divided in internal and external vibrations. Internal vibrations are due to the vehicle itself. The main sources are rotating parts: the wheels, the driveline and the engine. The main reason of these excitation is unbalance. External vibrations are due to the roughness of the road surface. It is important to study these excitations because they are responsible of the vertical load Fz at the tire-road contact. A large variation of Fz reduces the tire ability to exert forces in x and y direction. Generally, it is important to reduce vibrations that could cause discomfort, but at the same time, a complete suppression of excitation and noise could be undesirable and dangerous because they convey useful information to the driver and can give warnings in case of anomalies.

Road excitations cannot be studied using a deterministic approach because they are random signals and so must be treated using stochastic methods such as power spectral density (PSD). ISO 8608 divides road surfaces in 8 classes of power spectral density, from A to H [4]. Different studies have been conducted on the vibration perception of human body. ISO 2631 standard divides between vibrations that occur with a frequency that ranges between 0.5 Hz to 80 Hz that can cause discomfort and fatigue, and between vibrations that occur with a frequency that ranges between 0.1 Hz and 0.5 Hz that may cause motion sickness. The critical range of frequencies for human body is between 4 Hz and 8 Hz [5]. Natural frequencies of sprung and unsprung masses should be placed far from frequencies that produce discomfort. Lower natural frequencies, the ones linked to the sprung masses should be placed above 1 Hz to avoid motion sickness but below 4 Hz. Higher natural frequencies are due to unsprung masses motion and should be higher than 10-15 Hz [6].

In this paper the attention is focused on the multi-body modeling, on the virtual testing and on the correlation of simulation data with on-road tests data. The numerical model is very detailed and it is

characterized by rigid and flexible bodies, leaf and air springs and the FTire model concerning the tractor tires.

Handling analysis have been performed to check the goodness of the multi-body model performing standard maneuvers.

Comfort studies concern vibrations between 0 and 30 Hz and regard the correlation among experimental and simulated accelerations. Comfort analysis are performed on a Belgian block track; real and virtual test are performed in identical test conditions at different speeds and different loads, in order to check the fidelity of the virtual model with respect to the real truck. Therefore, the aim of the paper is a preliminary evaluation of the multi-body model response with respect to the on-road truck, performing the same track in the same test conditions. The numerical and experimental data are vertical accelerations measured on vehicle axles and frame. The signals correlation is carried out in frequency domain using Power Spectral Density (PSD) and in time domain using the level crossing peak counting (LC), a method especially used in durability and fatigue analysis.

Multi-body model

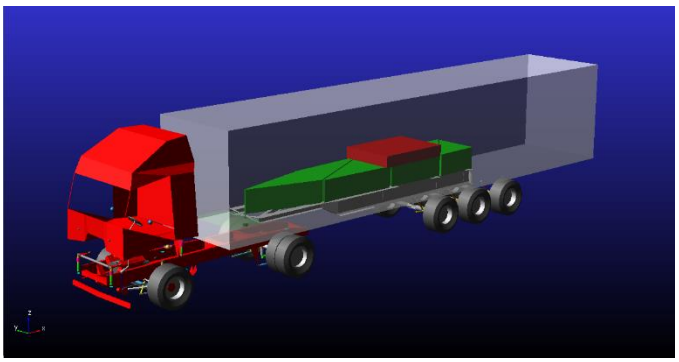

Figure 1. Heavy-duty truck multi-body model

The subject of this work belongs to heavy-duty truck category. Its load working rage is between 18 and 44 tons, the maximum allowed in European directives. It is characterized by a tractor and a semi-trailer, linked by means of a fifth wheel coupling. The tractor is composed by 2 axles and a suspended cabin. The front axle is steering while the traction comes from the rear one, which presents twinned wheels. The semi-trailer is characterized by three axles. Figure 1 shows the complete multi-body model, while the principal characteristics of the tractor and the semi-trailer are listed in Table 1 and Table 2.

N° of tractor axles	2
Traction	Rear axle
Steering axle	Front
Front suspension	Rigid axle, leaf spring
Rear suspension	Rigid axle, air springs, twinned wheels
Wheelbase	3,65 m
Track f / r	2,05 m / 1,82 m
Unladen tractor weight	7,5 tons
Engine	Diesel, 11,1L 6 cylinders (460CV)

Table 1. Tractor characteristics

N° of semi-trailer axles	3
Suspensions	Rigid axle, air spring
Fifth wheel-first axle distance	6,29 m
Axles distance	1,31 m
Total length	14,02 m
Unladen trailer weight	5,5 tons

Table 2. Semi-trailer characteristics

A complete CAD model was available for multi-body virtual vehicle model development. The latter is characterized by the following main subsystems:

- Cabin with dedicated suspension
- Tractor frame
- Engine
- Front suspension and steering system
- Rear suspension
- Semi-trailer
- Front/rear/semi-trailer wheels

Front suspension

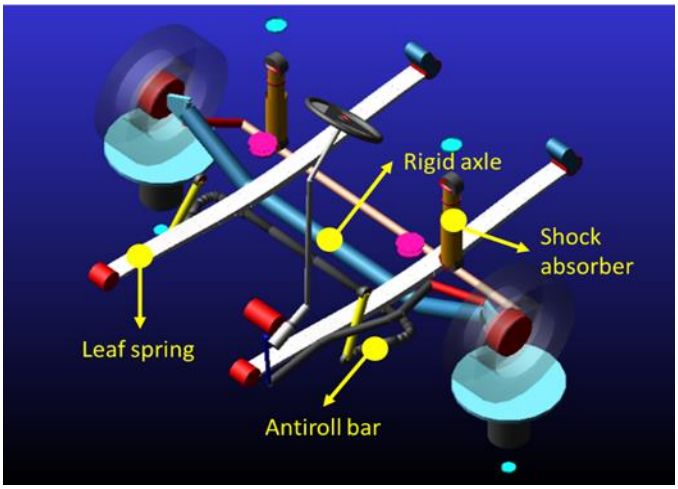

Figure 2. Front suspension and steering system

The principal task of a suspension system is to exchange static and dynamic forces between the vehicle and the road surface. Its major objective is to avoid the detachment of the wheels from the road surface and reduce the vibrations coming from road imperfections and roughness, improving comfort.

Figure 2 represents the tractor front suspension system. The front suspension system is of dependent type and is characterized by a rigid axle linking the two front wheels. It is connected to the chassis by means of two leaf springs, rigidly clamped to the top surface of the axle, two shock absorbers and the front antiroll bar. The antiroll bar is modeled as linear beam, it is flexible with distributed stiffness over the whole bar length. It is shaped like a cylindrical hollow bar, made of steel, curved and linked to the axle by means of two bushings and to the chassis by means of two rigid elements.

The primary component of the front suspension modelling is represented by the leaf springs which constitute an independent subsystem. The truck leaf spring is a mono-leaf with variable

thickness. It has been generated dividing the leaf in a series of rigid elements connected through Timoshenko beam elements; in this way the resulting model is flexible. Then the geometry of the leaves, the characteristics of the eyes, the shackle features and the material properties are defined. After that, it is possible to perform a static analysis, with which mechanical properties such as stiffness are checked. Then the preload can be set, and the leaf spring assembly created. The force vs displacement characteristic is linear in the considered working range, so the stiffness is constant.

Rear suspension

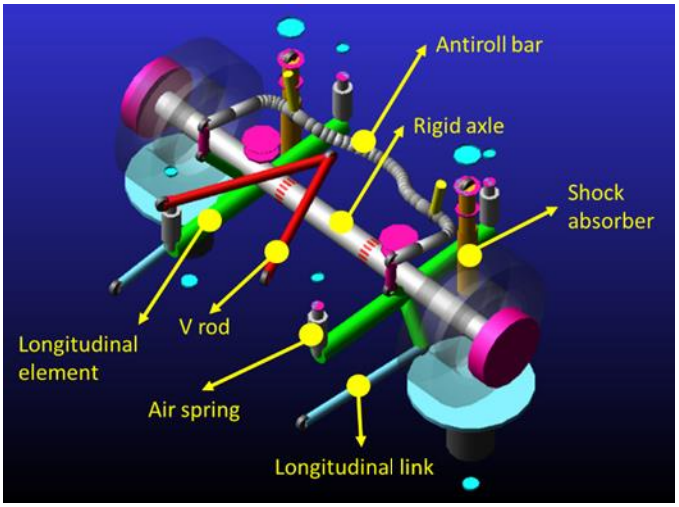

Figure 3. Rear suspension system

The rear suspension system is also of dependent type, but it is quite different respect the front one. Looking at Figure 3, it is characterized by a rigid axle that connects the rear twinned wheels. At the borders of this axle, two longitudinal elements are present. On these lasts a couple of air springs and a shock absorber link the axle to the truck frame. Another important component is the V rod that connects the rear axle to the chassis, constraining the motion of the suspension. Instead, two longitudinal links constrain the longitudinal motion. Finally, the rear antiroll bar modeled as a linear beam completes the rear suspension assembly.

Air springs are of rolling lobe type, very popular in commercial vehicles suspensions because of their low spring rate over a relatively large deflection range and their high static load carrying capability [1]. Figure 4 represents their force vs displacement characteristics at different pressure level as introduced in the model. These curves come from the interpolation by means of polytropic functions of the characteristics provided by the air spring manufacturer.

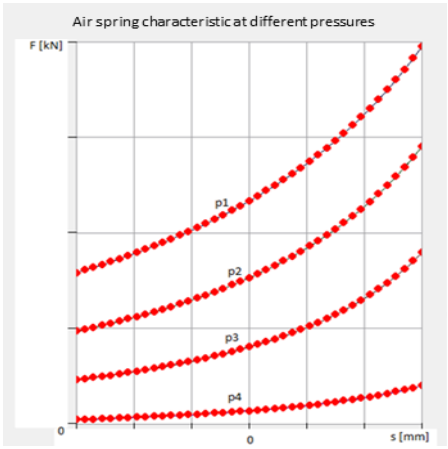

Figure 4. Air spring force vs displacement

Concerning shock absorbers, their force vs velocity characteristic is represented in Figure 5. These curves come from the data supplied by the shock absorber manufacturer. Their behavior is asymmetric and digressive, as typical for this component. The same considerations can be made for shock absorbers used for the rear suspension.

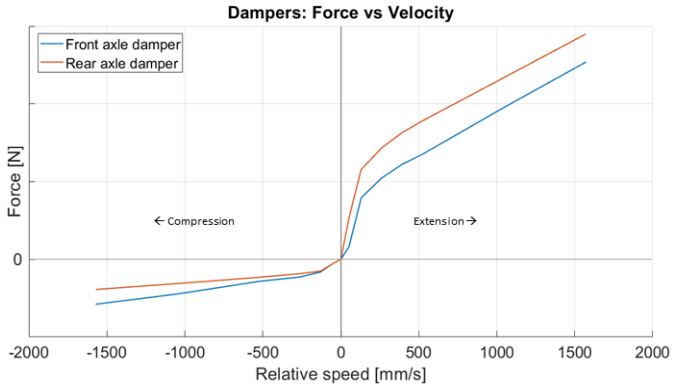

Figure 5. Shock absorbers force vs velocity characteristic

Semi-trailer suspension

The semi-trailer suspension is depicted in Figure 6. It consists of an axle, modeled like a linear beam, hinged into two longitudinal arms connected to the semi-trailer frame by a couple of shock absorbers and air springs.

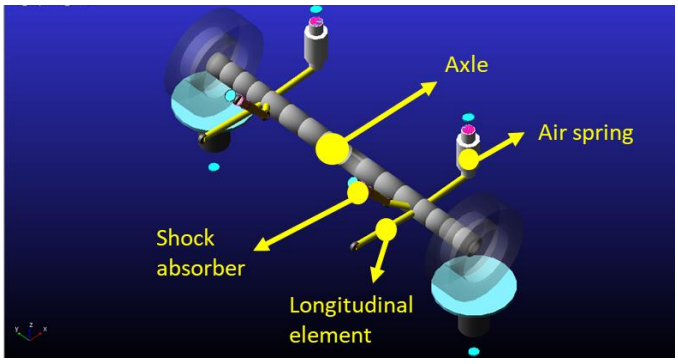

Figure 6. Semi-trailer suspension

Flexible bodies

Flexible bodies are present in the multi-body model under study. In fact, for large components subjected to heavy dynamic loads, is important to describe the correct behavior as far as stiffness and damping are concerned because they influence the whole mechanical assembly. This means that under dynamic loads the flexible body does not behave like a rigid element, but it deforms and vibrates. Flexible bodies are introduced in the simulation environment through files (.mnf - Modal Neutral File) containing the results of modal analysis of the bodies, i.e. the mode shapes and the natural frequencies of the part.

The flexible bodies present in the model are:

- Tractor frame
- Cabin
- Semi-trailer frame

Taking for example the tractor frame, the first four natural frequencies are in the frequency range considered for comfort studies. In fact, the first natural frequency is below 10 Hz, the second one between 10 and 20 Hz and the third and the fourth between 30 and 40 Hz. Figure 7 represents the first mode shape (torsional) of the chassis.

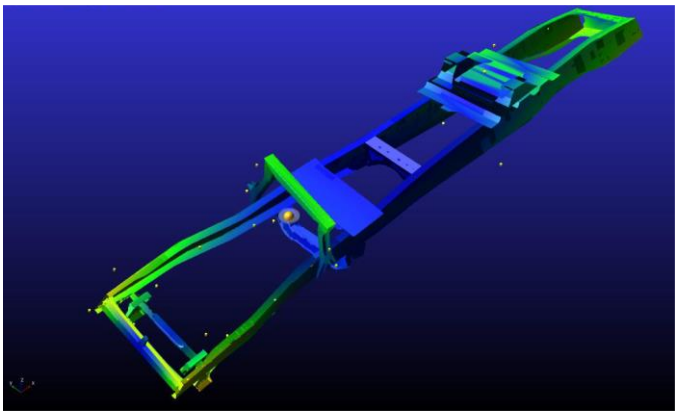

Figure 7. Tractor frame first mode shape

Tire model

Tire are responsible of the force exchanges between the vehicle and the road surface and they have the ability to filter out higher frequencies and reduce the forces transmitted to the suspension. With the need to have very predictable virtual models in the evaluation of ride comfort, the tire model plays a very important role. In this study FTIRE model is used for tractor tires. The acronym FTIRE means "Flexible Structure Tire Model" and it denotes a complete tool for tire dynamics simulation. It is a 3D nonlinear model that refers entirely to analytical means in order to reproduce tire behavior using classical mechanical and thermodynamic laws. FTIRE can be used for vehicle comfort simulations, prediction of road loads due to irregularities and for handling studies. It can be compared to a FEM model of the wheel and the contact between the tire and the road is not characterized by one point only but by a local contact patch pressure distribution. For these reasons the results coming from FTIRE model are very consistent and show very good correlation with experimental measures [7-9]. Due to the complexity of this model approach, simulations take significantly longer time respect the same simulation performed by PAC2002 tire model. During simulations, FTIRE model is able to take into account most of the aspects that characterize the tire on-road behavior, such as:

- the structural dynamics and belt dynamics
- frequency range up to 200 Hz due to road surface irregularities
- the thread wear, mass and stiffness imbalances and radius variation
- the distribution of the belt temperature
- the air volume vibration
- the tire slipping on the rim in case of large torques
- the flexible rim behavior
- the sidewall contacts

Road model

Beside having an accurate tire model, it is important to have high resolution road surface representations in order to perform realistic vehicle dynamics simulations. OpenCRG is a 3D representation of road surfaces. The acronym CRG, means "Curved Regular Grid" and it refers to the road description technique. This method has been developed and made available open source for everyone thanks to German companies. It is characterized by a "Curved Reference Line" that is the representation of the road map in the global coordinate system (*x-y* axis). The global reference system is transformed in a grid, the "Regular Elevation Grid" that is described by the *u* axis, which coincides with the reference line, and the *v* axis that is perpendicular to *u* axis. Each grid cell contains height information completing the road surface description with the longitudinal and the transversal road slope. The data necessary for this model to precisely describe the road surface can be obtained thanks to laser scanning. To this purpose, vehicles with high-resolution equipment for road surface measurement are used [10-12].

Figure 8 shows the virtual environment 3D visualization of the Belgian block track performed by the on-road vehicle during comfort tests. It has been laser scanned and the surface obtained using OpenCRG technique and format. It has a very detailed resolution of 1x1x0.1 cm in *x-y-z* directions.

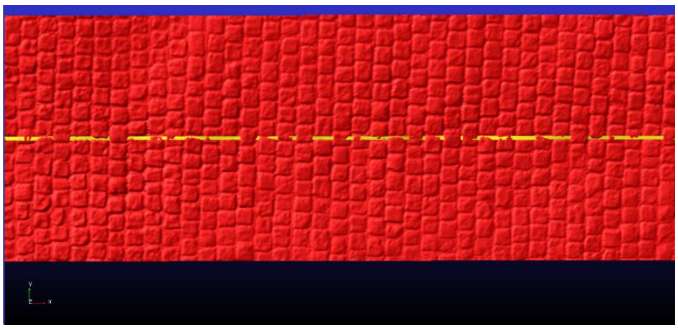

Figure 8. 3D road model of the Belgian block track

Load conditions

In order to meet real on-road test conditions, the load distribution is properly tuned. To this purpose four ballast have been created on the tractor flexible chassis, in correspondence of the interface nodes between the shock absorbers and the frame. In this way it is possible to obtain a correct weight distribution between left and right wheels

and front and rear axles. In Table 3 and Table 4 are summarized the load conditions.

Unladen condition [tons]	
Front axle	4,75
Rear axle	2,80
Total weight	7,55

Table 3. Unladen condition

Laden condition [tons]			
Front axle	6,80		
Rear axle	11,20		
Semi-trailer axles	3,85	3,85	3,85
Total weight	29,55		

Table 4. Laden condition

The unladen condition concerns the tractor only with the driver and a passenger, each one weighing 75 kg. The laden condition concerns the tractor with the driver and a passenger, each one weighing 75 kg, the semi-trailer and the load, for a total load of 29,55 tons. Pacejka's tire models are used for the tractor and the semi-trailer for handling maneuvers, while for comfort analysis FTIRE model is introduced for the tractor.

Handling simulations

In this section handling simulations are presented. Before proceeding with tests that are object of this study, let us investigate if the vehicle behaves correctly performing standard lateral dynamics maneuvers. Three kind of test are performed: ramp steer, sweep steer and step steer. These maneuvers are normed by ISO standards for passenger vehicles. In the case under analysis, standards are adapted to heavy-duty vehicles limits [13,14].

Handling maneuvers have been performed with the two vehicle configurations used for the comfort analysis: the unladen (tractor only) and the laden (tractor, semi-trailer and load) conditions. The test settings are maintained the same for the two load cases. All the quantities are evaluated at the tractor center of gravity.

Ramp steer

This test is performed at 60 km/h by applying a steering input that constantly increases with time, at a rate of 10 deg/s. During the test, accelerator pedal is kept constant, although in this way the vehicle speed decreases during the steering event, in order to avoid large longitudinal forces at high lateral accelerations. The maneuver ends when the test limit condition is achieved, i.e. when the vehicle loses adherence or becomes unstable. In the laden condition, the vehicle limit condition consists in the spin of the tractor that rotates around the fifth wheel and hits the semi-trailer.

The principal results are plotted in function of the lateral acceleration.

Figure 9 represents the tractor curvature of the two conditions. It is possible to see that above 0.45 g of lateral acceleration, the curvature increases more rapidly for the laden condition, if compared with the unladen one, because of the presence of semi-trailer.

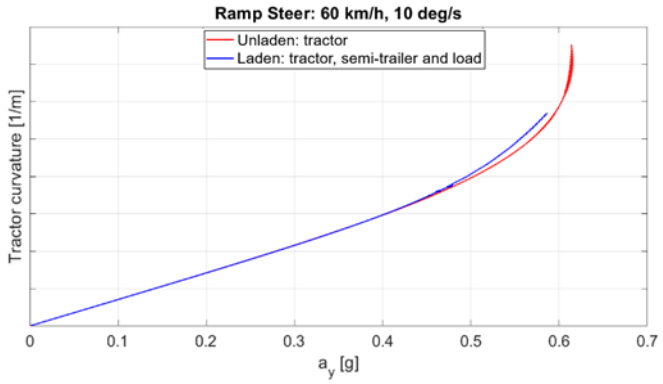

Figure 9. Ramp steer: Tractor curvature

Figure 10 shows the dynamic steering wheel angle as a function of the lateral acceleration. It is possible to see that for low and medium lateral accelerations both the configurations have understeering behavior while at limit condition they become oversteering. For the unladen vehicle the oversteering condition is suddenly reached at high lateral acceleration. For the laden vehicle, the understeering gradient above 0.3 g starts to increase before changing sign, thus giving a feedback to the driver that the maximum acceleration is becoming closer.

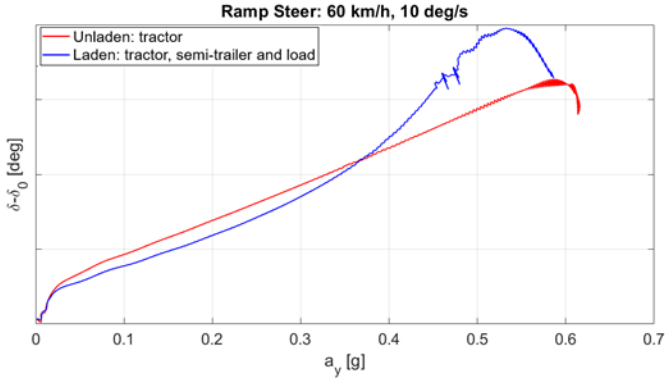

Figure 10. Ramp steer: dynamic steering wheel angle vs lateral acceleration

Figure 11 shows the dynamic sideslip angle versus lateral acceleration: it keeps lower in modulus for the unladen condition at high lateral acceleration, while for laden condition it starts to increase rapidly over 0.45 g following a vertical asymptote at 0.6 g.

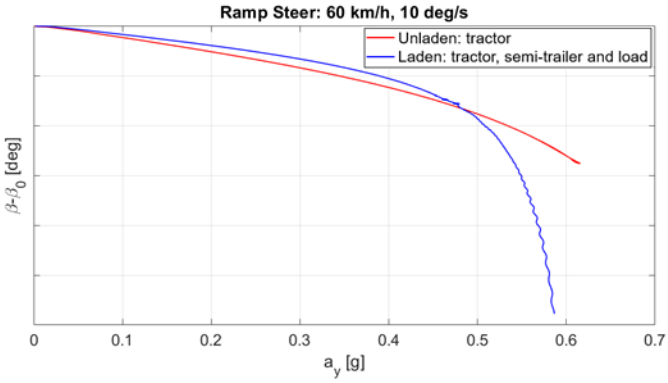

Figure 11. Ramp steer: dynamic sideslip angle vs lateral acceleration

The yaw rate increases linearly with lateral acceleration, as could be seen in Figure 12. This behavior can be considered equal for both the configurations until 0.45 g, then in the laden condition it increases rapidly because of the spin of the tractor for the semi-trailer influence.

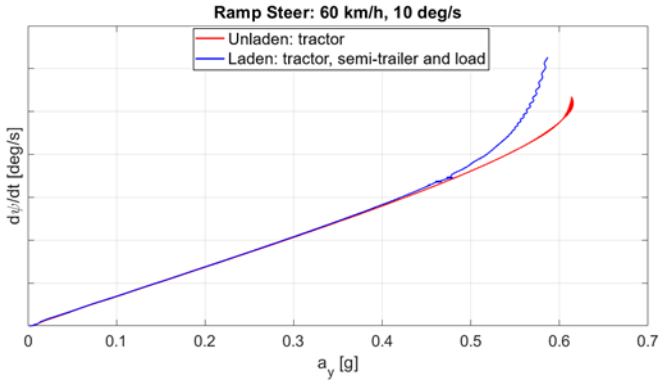

Figure 12. Yaw rate vs lateral acceleration

Step steer

Step steer is performed at 70 km/h maintaining the throttle constant during the maneuver. It is characterized by a steering input suddenly applied and then maintained in order to evaluate the transient behavior of the vehicle. The steering input must be very fast: 0.15 s and its amplitude fixed and corresponding to the steering angle that, in a steady-state lateral test, provides a certain lateral acceleration. In this case, it has been chosen 50 degree. It is important to verify that the vehicle does not rollover performing this test.

The principal results are plotted as functions of time.

In Figure 13 is possible to notice the lateral acceleration behavior of the two configurations. The oscillation at high frequency between 5 and 5.5 seconds is due to the engine suspension movement immediately after the steering input application. The trend of the curve at low frequency between 5.5 and 8 seconds is due to the cabin roll, allowed by its suspension system. It can be seen that the lateral acceleration, after reaching the maximum value, starts to decrease because of the speed reduction during the maneuver.

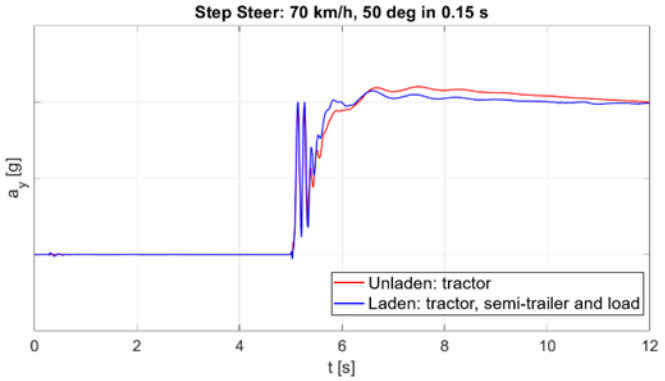

Figure 13. Step steer: Lateral acceleration vs time

In Figure 14 is possible to notice the roll angle behavior of the two configurations. The laden configuration achieves higher roll angle values. The trend of the curve at low frequency between 5.5 and 8 seconds is due to the cabin roll, as said before. Also in this case, after reaching the maximum value, the trend of the curves is decreasing due to the reduction in speed during the maneuver. It is clear that in this test, that can be considered similar to an emergency maneuver, the rollover it is not reached for both the configurations.

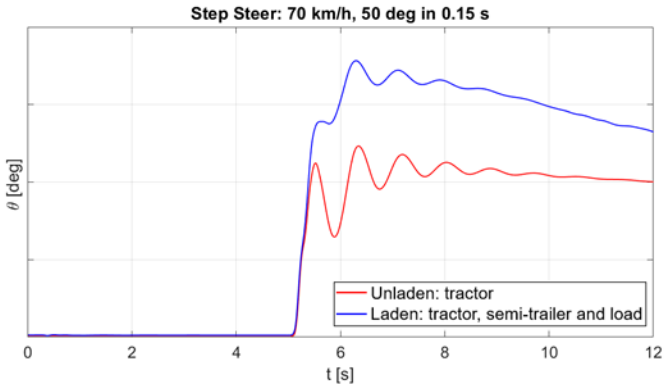

Figure 14. Step steer: Roll angle vs time

Sweep steer

This test is performed at 60 km/h and it consists in a continuous sinusoidal steering input. Even in this case the throttle is maintained constant despite the speed decrease during the maneuver. The steering amplitude is fixed and corresponds to the steering angle that, in a steady-state lateral test, provides a certain lateral acceleration. In this case it has been chosen 50 deg. The steering frequency is continuously increased, starting from 0.2 Hz up to 2 Hz.

The principal results are plotted using Bode diagrams as a function of the excitation frequency.

In the following diagrams the gain, which gives information about the amplitude of the response, and the phase, which impacts the delay time of the response, are plotted.

Figure 15 shows the roll angle response to the input lateral acceleration, in frequency domain. It is possible to see that at low frequencies the gain of the roll angle is lower for the unladen condition. Instead, at medium frequencies a higher peak value is present for unladen with respect the laden vehicle. The phases remain very similar for all the frequency range.

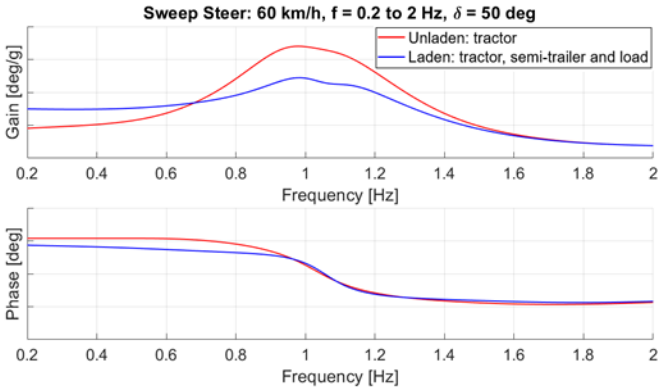

Figure 15. Sweep steer: roll angle/lateral acceleration

Experimental set-up for comfort analysis

A total of ten accelerometers have been positioned in order to record vibrations during Belgian block track tests. Two have been located on the front axle near the interconnection with the leaf springs. Other two are situated on the rear axle near the hubs. Four accelerometers are placed on the tractor frame near the link with the four shock absorbers. The last two have been positioned at the seat attachment and on the seat pad. Output data coming from accelerometers have been stored, filtered and down-sampled at 100 Hz in agreement with the virtual simulations environment sampling frequency. Signals are recorded in time domain and transformed in frequency domain in order to be compared with signals coming from simulation environment.

Concerning the multibody model, accelerations have been recorded in the same positions as the real accelerometers of the on-road test track. The seat pad signal is not recorded because the seat suspension and the seat itself are not modeled. Figure 16 shows accelerometer positioning.

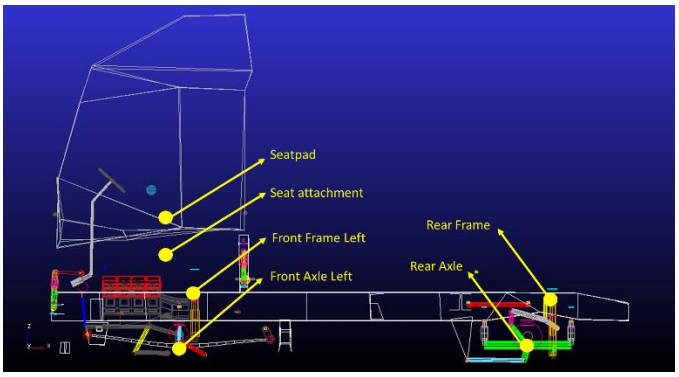

Figure 16. Accelerometer positioning

Test conditions

Belgian block is one of the hardest tracks used for testing comfort and durability of a vehicle. In fact, it is part of the hundreds of tests that are performed during vehicle development. In this type of track, due to high accelerations, it is possible to evaluate ride comfort, NVH, bolt tightening resistance, interior and exterior parts resistance, components durability and other vehicle critical issues. Consequently, this kind of test is of fundamental importance in order to correlate the multibody model with the real vehicle. Four different tests will be discussed in this paper, one performed in "unladen" condition (only the tractor) and three in "laden" condition (tractor, semi-trailer and load):

- Unladen test has been performed at 40km/h, at constant speed;
- Laden tests have been performed:
  - at 40 km/h, at constant speed;
  - at 45 km/h, at constant speed;
  - from 15 to 30 km/h with constant acceleration.

Experimental-numerical correlation

Power Spectral Density

In this section the correlation of the numerical and experimental data, concerning the comfort analysis, is presented. The vertical accelerations, recorded by real accelerometers on track and by virtual sensors positioned in the multibody model, will be compared in terms of power spectral density (PSD). The PSD is a typical tool for vibration analysis of random signals [15-19].

In particular, the power spectral density estimate of the acceleration signals is found using Welch's overlapped segment averaging estimator, which is implemented in a dedicated Matlab function. The parameters used are the followings:

- Sampling frequency: 100 Hz
- Number of frequency points on the spectrum: 2048
- Windows type: Hanning
- Windows segment length: 512
- Overlap: 50%

Root Mean Square

The root mean square (RMS) of the signals is computed in order to quantify the total power of a signal and it was used to verify the filtering effect at each suspension system. The root mean square for a discrete signal is defined as:

$$x_{rms} = \sqrt{\frac{1}{n}\sum_{i=1}^{n} x_i^2} \qquad (1)$$

Where:

- x_{rms} : root mean square
- x_i : i^{th}-sample
- n : total number of samples

Level Crossing Peak Counting

An alternative representation of the correlation, using level crossing peak counting (LC), will be given. This technique is widely used in telecommunication field and it is a method adopted in the aeronautical industry to count, in a simple way, accelerations that exceeded certain discrete levels. Moreover, it is widely used in durability and fatigue analysis in order to evaluate the consistency of the loads versus the number of occurrences. The number of times a defined acceleration level is crossed is reported on the *x*-axis in logarithmic scale, while on the *y*-axes are the vertical acceleration levels crossed by the signal.

Results

The results shown in this section concern one truck configuration and two quarters of the vehicle. The unladen condition with tractor only (without trailer) is considered, the road is a Belgian block track and the test is performed at an almost constant speed of 40 km/h. The two quarters of the vehicle analyzed are front right and rear left.

Figures from 17 to 21 represent the experimental and simulation results obtained from the accelerometers positioned on the front right side of the vehicle.

The typical frequency range considered in comfort analysis and also evaluated for this study is between 0 and 30 Hz.

Figure 17 represents the power spectral density of the experimental signals recorded from the front axle right accelerometer, the red curve, to the seat pad accelerometer, the magenta curve. At low frequencies (around 2 Hz) the power content of the frame signal, the seat attachment signal and the seat pad signal are higher than the one recorded by the front axle. This means that at low frequencies there is an amplification effect. At frequencies higher than 5 Hz, it is possible to notice that the power of the signal is decreasing passing from the axle to the seat. This means that there is a filtering effect at each stage. Looking at the red and the blue curve, it is possible to see the filtering of the front suspension, between the blue curve and the black one, the filtering of the cabin suspensions, and finally between the black and the magenta curves the seat suspension effect. This means that the vibrations power perceived at each stage, gradually decreases passing from the road to the driver.

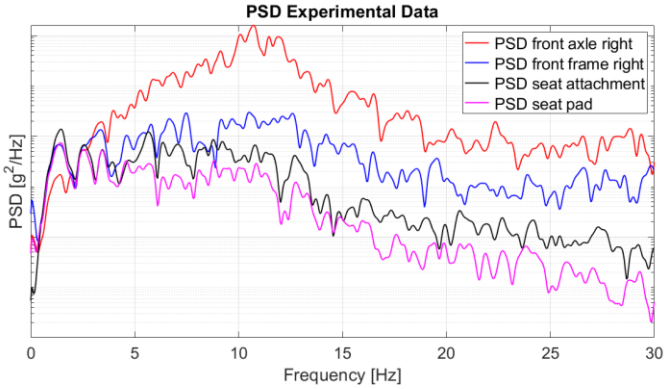

Figure 17. PSD of front right side experimental data

Figure 18 represents the power spectral density of the simulation signals recorded from the front axle right accelerometer, the red curve, to the seat attachment accelerometer, the black curve. As said before, the seat pad signal is not available because the seat suspension and the seat pad are not modeled in multibody environment. As it happens in experimental results, at low frequencies (around 2 Hz) the power content of the frame signal and the seat attachment signal are higher than the one recorded by the front axle. This means that at low frequencies there is an amplification effect. At frequencies higher than 5 Hz, it is possible to notice that the power of the signal is decreasing passing from the axle to the seat attachment. This means that there is a filtering effect at each stage. Looking at the red and the blue curve, it is possible to see the filtering of the front suspension and between the blue curve and the black one, the filtering of the cabin suspensions.

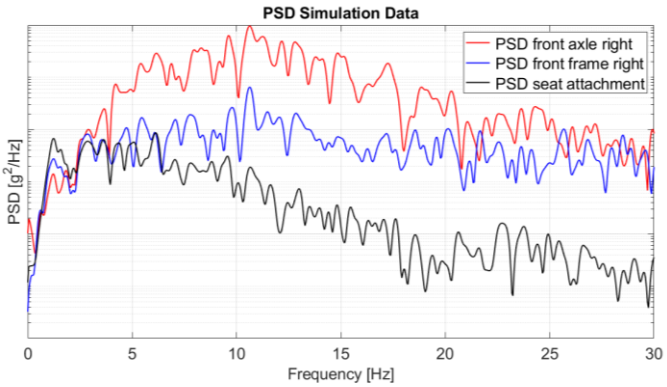

Figure 18. Front right side PSD comparison of simulation results

Figure 19 represents the correlation between the experimental and simulation results in terms of root mean square. From this graph it is possible to notice in a better way the vibration energy content decrease, passing from the axle to the seat. Moreover, it is also possible to verify the goodness of the multibody model, because looking at the bars with the same color, the delta between the experimental and the simulation RMS is very low.

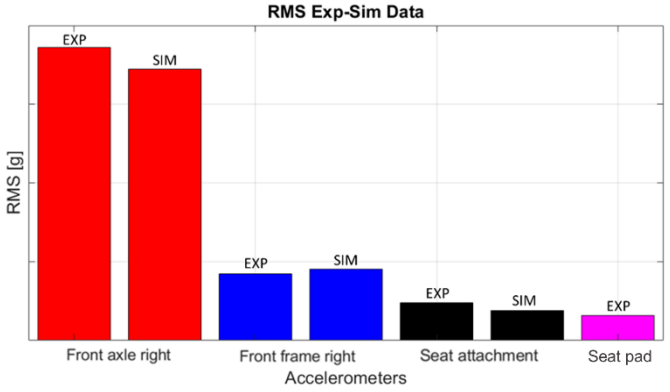

Figure 19. Front right side RMS experimental-simulation comparison

Figure 20 and 21 show the level crossing peak counting correlation. As seen in previous analysis, with LC we have a further confirmation of the filtering effect passing from the road to the driver. This means that the higher accelerations are recorded on the axle, while the lower on the seat pad.

Figure 20 represents the LC plot of experimental data.

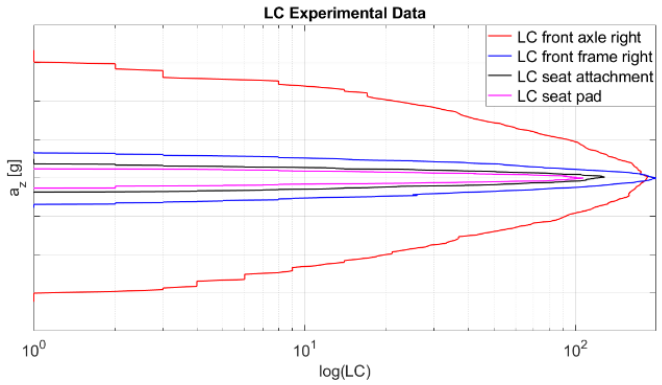

Figure 20. Front right side LC comparison of experimental results

Figure 21 represents the LC plot of simulation data.

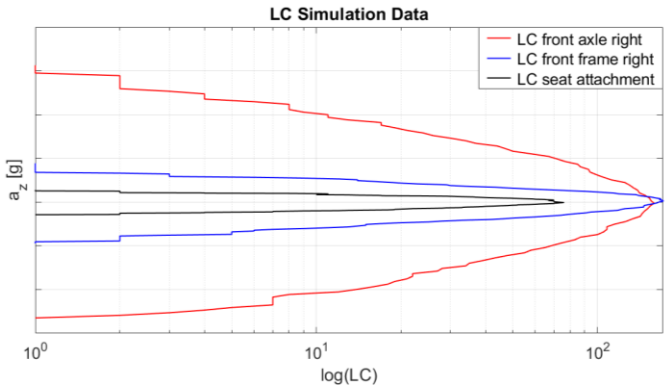

Figure 21. Front right side LC comparison of simulation results

Considering that the y-axis scales are similar for the two graphs, there is a very good correlation between experimental and simulation results, also considering the amplitude of the accelerations recorded.

Figures from 22 to 26 represents the experimental and simulation results obtained from the accelerometers positioned on the rear side of the vehicle.

Figure 22 shows that at low frequencies (around 2 Hz) the power content of the frame signal, the seat attachment signal and the seat pad signal are higher than the one recorded by the rear axle. This means that at low frequencies there is an amplification effect. At frequencies higher than 5 Hz, it is possible to notice that the power of the signal is decreasing passing from the axle to the seat. This means that there is a filtering effect at each stage. Looking at the red and the blue curve, it is possible to see the filtering of the front suspension, between the blue curve and the black one, the filtering of the cabin suspensions, and finally between the black and the magenta curves the seat suspension effect. At frequencies higher than 23 Hz the blue curve (PSD of the rear frame left) is higher than the red one (PSD of the rear axle) showing an amplification effect of the rear suspension at higher frequency.

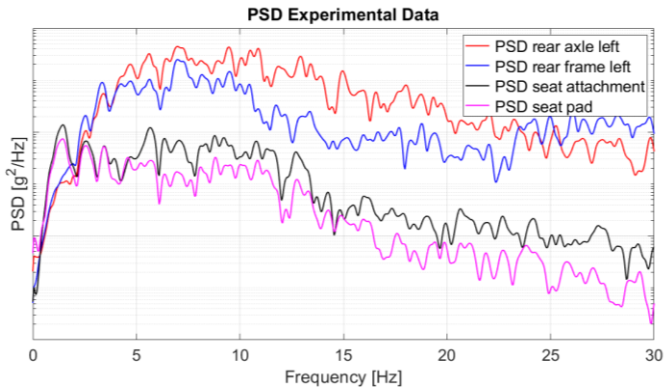

Figure 22. Rear left side PSD comparison of experimental results

Figure 23 represents the power spectral density of the simulation signals recorded from the rear axle left accelerometer, the red curve, to the seat attachment accelerometer, the black curve. As it happens in experimental results, at low frequencies (around 2 Hz) the power content of the frame signal and the seat attachment signal are higher than the one recorded by the front axle. This means that at low frequencies there is an amplification effect. At frequencies higher than 5 Hz, it is possible to notice that the power of the signal is decreasing passing from the axle to the seat attachment. This means that there is a filtering effect at each stage. Looking at the red and the blue curve, it is possible to see the filtering of the front suspension and between the blue curve and the black one, the filtering of the cabin suspensions. In this case the frame PSD does not overcome the axle one over 23 Hz, as it happens in simulation results. This means that there is not a very good correspondence between the rear suspension of the multibody model and the real one.

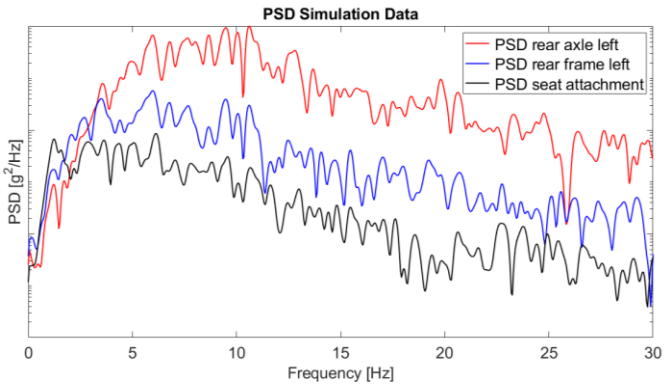

Figure 23. Rear left side PSD comparison of simulation results

Figure 24 represents the correlation between the experimental and simulation results root mean square. From this graph it is possible to notice in a better way the vibration energy content decrease, passing from the axle to the seat. Moreover, it is also possible to verify the goodness of the multibody model. In this case the differences are bigger than in the previous case (front axle right side). The most important difference concerns the filtering effect of the rear suspension. In experimental results it is possible to notice a lower filtering effect if compared with the filtering effect obtained in the multi-body model. This situation can be due to the elastic characteristic of the air springs. In fact, the polytropic curve used to model their behavior in the multi-body environment has been fitted for little displacements, while for big displacements the air spring curves adopted are not very accurate.

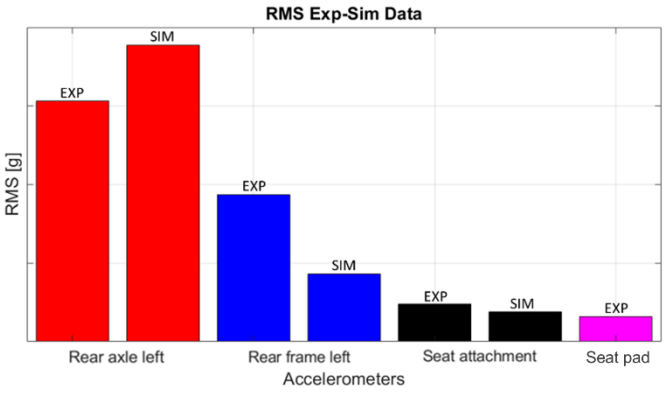

Figure 24. Rear left side RMS experimental-simulation comparison

Figure 25 and 26 show the level crossing peak counting correlation. As seen in previous analysis, with LC we have a further confirmation of the filtering effect passing from the road to the driver. This means that the higher accelerations are recorded on the axle, while the lower on the seat pad.

Figure 25 represents the LC graph of experimental data.

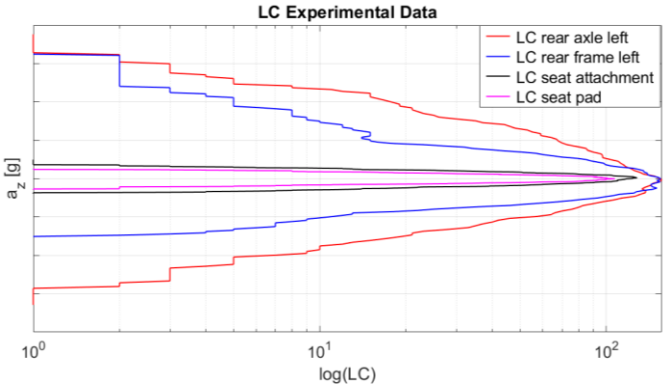

Figure 25. Rear left side LC comparison of experimental results

Figure 26 represents the LC graph of simulation data.

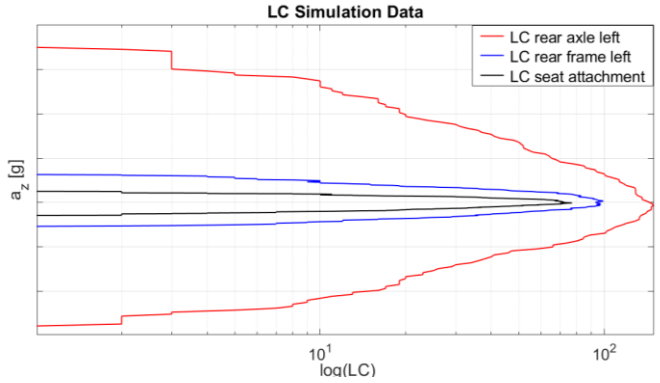

Figure 26. Front right side LC comparison of simulation results

Considering that the y-axis scales are the same for the two graphs, there is a good correlation between experimental and numerical accelerations recorded on the rear axle. A remarkable difference can be seen comparing the curves of the frame (blue curves). In fact, experimental accelerations of the rear frame have higher values with respect to the simulation ones. This fact confirms what it has been already said while analyzing RMS bar plot.

Conclusions

In this paper, the study of the correlation between numerical and experimental comfort analysis of a heavy-duty vehicle was presented. The study is carried out through experimental tests (Belgian block track) and numerical simulations in order to evaluate tires and suspension systems behavior of the multibody model respect the on-road truck.

The output data coming from the numerical and the experimental tests are vertical accelerations in time domain, registered by ten accelerometers positioned on the axles, the chassis and the cabin of the truck.

The numerical simulations have been performed reproducing the real test conditions (speed, tire inflation pressure, load distribution, etc.) on the 3D reproduction of the Belgian block track using a complete multibody model of the truck.

The correlation has been conducted using three different techniques, typical of non-deterministic signals: the power spectral density (PSD), the root mean square (RMS) and the level crossing peak counting (LC).

The obtained results are promising, considering that these are the first outcomes obtained without tuning the model parameters and characteristics. The best outcomes concern the correlation of the front right quarter of the vehicle while for the rear left one some model adjustments are needed.

The preliminary results presented in this paper constitutes a starting point for sensitivity analysis and parameter tuning of the multibody model.

The validated multi body model can be used to improve handling, comfort and durability of future heavy-duty vehicles.

References

1. Anderson, D., Schade, G., Hamill, S., and O'Heron, P., "Development of a Multi-Body Dynamic Model of a Tractor-Semitrailer for Ride Quality Prediction," SAE Technical Paper 2001-01-2764.
2. Shaik Mohamad, A., Vijayakumar, R., and rao.P, N., "Vibroacoustic Optimization of Tractor Cabin and Correlation with Experimental Data," SAE Technical Paper 2017-01-1847.
3. Jain, A. K., Madaswamy, S., Sudarsanam, S., and Srinivas, V., "Assessment of Ride in a Heavy Commercial Truck Using Numerical Simulation Methods and Correlation with Test," SAE Technical Paper 2013-26-0151.
4. International Organization for Standardization, ISO 8608:2016, "Mechanical vibration — Road surface profiles — Reporting of measured data," International Organization for Standardization (2016).
5. International Organization for Standardization, ISO 2631-1:1997, "Mechanical vibration and shock — Evaluation of human exposure to whole-body vibration," International Organization for Standardization (1997).
6. Fichera, G., Scionti, M., and Garescì, F., "Experimental Correlation between the Road Roughness and the Comfort Perceived In Bus Cabins," SAE Technical Paper 2007-01-0352.
7. Dorfi, H. R., "Tire Cleat Impact and Force Transmission: Modeling Based on FTIRE and Correlation to Experimental Data," SAE Technical Paper 2004-01-1575.
8. Gipser, and Hofmann, "FTIRE - Flexible Structure Tire Model Modelization and Parameter Specification," Cosin Scientific Software documentation.
9. Gipser, M., "FTIRE, a New Fast Tire Model for Ride Comfort Simulations," International ADAMS User Conference Berlin 1999.
10. Borse, R. H., "Analysis, creation and extraction of three-dimensional road profiles using open CRG tool", International Engineering Research Journal (IERJ), ISSN 2395-1621.

11. Potó, V., Csepinszky, A., and Barsi, Á., “Representing road related laserscanned data in curved regular grid: a support to autonomous vehicles,” The International Archives of the Photogrammetry, Remote Sensing and Spatial Information Sciences Volume XLII-2, 2018.
12. OpenCRG, “User manual”, VIRES Simulationstechnologie GmbH (2017) VI2009.050.
13. International Organization for Standardization, ISO 4138:2004, “Passenger cars - Steady-state circular driving behavior – Open-loop test method,” International Organization for Standardization (2004).
14. International Organization for Standardization, ISO 7401:2003, “Road vehicles – Lateral transient response test methods – Open-loop test method,” International Organization for Standardization (2003).
15. Londhe, A., Kangde, S., and Moorthy, N., "Evaluation of Vehicle Systems Structural Durability Using PSD Based Fatigue Life Approach," SAE Technical Paper 2012-01-0953.
16. Wang, D., Hao, H., Zhang, B., and Chen S., "Simulation and Test in Virtual Prototype of Heavy-duty Truck with Full-floating Cab and Air Suspension," ICCDA 2010 978-1-4244-7164-5.
17. Yang, Y., Ren, W., Chen, L., Jang, M. et al., “Study on ride comfort of tractor with tandem suspension based on multy-body system dynamics,” Science Direct, Applied Mathematical Modelling 33 (2009) 11-33.
18. Lu, Y., Yang, S., Li, S., Chen, L., “Numerical and experimental investigation on stochastic dynamic load of a heavy duty vehicle,” Science Direct, Applied Mathematical Modelling 34 (2010) 2698-2710.
19. Greco, P. C., de Barcellos, C. S., and da Rosa Neto, A “A Numerical Model for Passenger Car Ride Comfort Studies,” SAE Technical Paper 2001-01-0039.

Contact Information

enrico.galvagno@polito.it

Definitions/Abbreviations

PSD	Power spectral density
RMS	Root mean square
LC	Level crossing peak counting
NVH	Noise vibration and harshness
TCO	Total cost of ownership
CRG	Curved regular grid
FTIRE	Flexible structure tire model
FEM	Finite element method
δ	Steering wheel angle
δ_0	Kinematic steering wheel angle
β	Side slip angle
β_0	Kinematic side slip angle
Θ	Roll angle
Ψ	Yaw angle
a_y	Lateral acceleration
a_z	Vertical acceleration